PHYSICAL REVIEW A

ATOMIC, MOLECULAR, AND OPTICAL PHYSICS

RAPID COMMUNICATIONS

The Rapid Communications section is intended for the accelerated publication of important new results. Since manuscripts submitted to this section are given priority treatment both in the editorial office and in production, authors should explain in their submittal letter why the work justifies this special handling. A Rapid Communication should be no longer than 4 printed pages and must be accompanied by an abstract. Page proofs are sent to authors.

Complete photofragmentation of the lithium atom

A. W. Malcherek, J. M. Rost, and J. S. Briggs

Theoretische Quantendynamik, Fakultät für Physik, Universität Freiburg, Hermann-Herder-Strasse 3, D-79104 Freiburg, Germany

(Received 7 February 1997)

Differential cross sections describing the correlated motion of three electrons in the nuclear Coulomb field during the complete photofragmentation of a four-body system, the lithium atom, are calculated. Two selection rules are derived and their operation illustrated. Two features, not present in the corresponding three-body case are emphasized, namely that the Wannier configuration, in contrast to the three-body photofragmentation of helium, is allowed. Second, the cross section to access certain spin-momentum configurations of the three particles is zero for an uncorrelated but finite for a correlated final state. [S1050-2947(97)50406-9]

PACS number(s): 32.80.Fb, 41.60.Ap

The correlated motion of slow electrons moving in the field of a positive ion is one of the most studied problems of recent years in atomic physics. Such states are produced as the final states in the breakup of collision complexes or following photon absorption. As such they are prime examples for the study of the multiple fragmentation of highly excited systems in general. The simplest examples are the photo-double-ionization of helium [the $(\gamma,2e)$ process] and the electron-impact ionization of the hydrogen atom [the $(e,2e)$ process]. These fundamental, fully fragmented three-body Coulomb systems have been studied not only to ascertain the Wannier-threshold law [1] but also to determine the multiply differential cross section for emission of the two electrons with specified momenta $\vec{k}_1$ and $\vec{k}_2$ [2].

The corresponding simplest examples in the case of three continuum electrons are the photo-triple-ionization of lithium [the $(\gamma,3e)$ process] and the electron-impact double-ionization of helium [the $(e,3e)$ process]. Although coincidence experiments exist in the latter case, they are only for high-energy scattered electrons where the dynamics are essentially those of the $(\gamma,2e)$ process (momentum transfer tends to zero). Accordingly, earlier theories [3] of this process ignore the correlation of the fast electron motion to that of the other two. In the case of the $(\gamma,3e)$ process, only the energy dependence of the total cross section near threshold

has been measured and shown [4] to agree with the dependence predicted by ''Wannier theory.''

Here we present theoretical multiply differential cross sections in which the correlated motion of all three electrons is taken into account. Specifically we consider the complete four-particle fragmentation of the lithium atom from its $(1s^2 2s\ {}^2S^e)$ ground state by the absorption of a single photon. In the final state the electrons $j=1,2,3$ are emitted with well-defined momenta $\vec{k}_j$ and spin orientation. Furthermore, we generalize some results for the $(\gamma,2e)$ process [5] to establish selection rules [incidentally, also valid for $(e,3e)$ processes] for emission into certain $(\vec{k}_1,\vec{k}_2,\vec{k}_3)$ combinations. Although triply excited states of Li have been observed [6], attempts to measure three continuum electrons in coincidence have so far proved fruitless [7]. Nevertheless, recent technological advances in synchrotron light source brightness and the development of techniques such as recoil-ion spectroscopy [8] give grounds for optimism that the coincidence detection of four-particle fragmentation may soon be realized. In this case the selection rules established here provide a guide to experimenters to avoid configurations where the cross section is zero due to symmetry conditions.

For double photoionization, the dominant mode of emission near threshold is in the ''back-to-back'' configuration (relative angle between the two electrons is $\Theta_{12}=180°$), i.e., the Wannier mode. Unfortunately, in helium the ${}^1P^o$ symmetry of the final state implies that emission into this con-

figuration is forbidden [9], so that direct observation of the Wannier mode is not possible. The analogous mode for three electrons is when the electrons emerge in plane at relative angles $\Theta_{12} = \Theta_{23} = \Theta_{31} = 120°$. Here we show that for triple photoionization of lithium ($^2S^e \to {}^2P^o$), this Wannier configuration is allowed. Furthermore, the symmetric configuration shows a maximum with respect to angular variation of the Θ_{ij} around it.

In addition to the above difference between the two-electron and three-electron photoionization processes there is also an aspect that arises concerning spin. In the photoionization of helium, only a spin singlet occurs, so that the continuum state has one electron in the spin-up state and one in the spin-down state. In lithium, however, we have a spin doublet, with one electron having a spin orientation opposite the other two. As shown below, even when the electrons are emitted symmetrically to the beam and with equal energies, there is a dependence of the cross section on the disposition of the electron pair with equal spin orientation to the third electron.

An experiment is visualized in which three electrons are detected in coincidence and their energies, directions of emission, and spin orientation are measured. For fixed photon energy, only the energies of two of the electrons need to be measured and the cross section is

$$\frac{d\sigma}{d\Omega_1 \, d\Omega_2 \, d\Omega_3 \, dE_1 \, dE_2} = 4\pi^2 \alpha \frac{k_1 k_2 k_3}{\omega} |V_{fi}|^2, \quad (1)$$

where the dipole matrix element is

$$V_{fi} = \omega \left\langle \Psi_f(\vec{k}_j, s_j) \middle| \hat{\epsilon} \cdot \sum_j \vec{r}_j \middle| \Psi_i(s_j) \right\rangle. \quad (2)$$

The final state Ψ_f specifies the final momentum $\vec{k}_j$ and spin state s_j (spin up or down) of each electron $j = 1,2,3$. If the individual spin orientations are not detected, then a suitable average must be performed over the alternative spin states. The light polarization vector is $\hat{\epsilon}$ (here we consider linear polarization only).

In LS coupling the initial state has quantum numbers $L'S'\pi'$, where π' is the parity. The dipole selection rules then limit the final state to a few values of $LS\pi$. Whether a given three-electron continuum state $|LS\pi\rangle$ contributes to the measured cross section depends upon whether the overlap matrix element $\langle \vec{k}_1 s_1, \vec{k}_2 s_2, \vec{k}_3 s_3 | LS\pi \rangle$ is zero or not. In analogy to the expansion of the two-electron wavefunction into bipolar harmonics [5], the three-electron wave function can be expanded in tripolar harmonics. Using the properties of these harmonics, we have derived two selection rules. They are both generalizations of selection rules established for two electrons (in fact they are valid for any number of electrons). The first is the generalization of selection rule A of [5].

Selection rule A: If all electrons are emitted in a plane perpendicular to the $\hat{z}$ axis of quantization, then the $M = 0$ component does not contribute to the cross section for π odd.
The second is a generalization of selection rule J of [10].

Selection rule J: If all electrons and the quantization axis $\hat{z}$ lie in a plane, then states with $M = 0$ and $\pi + L$ odd do not contribute to the cross section.

In the case of photoionization the $\hat{z}$ axis will be taken to be the photon polarization direction $\hat{\epsilon}$.

The full photofragmentation cross section of lithium has been evaluated by calculating the nine-dimensional integral involved in the transition matrix element by direct numerical integration using a Monte Carlo method that is based on the algorithm VEGAS [11].

In order to analyze the structure of the cross section, various approximate wave functions have been used. The ground state has been taken to be the single Slater determinant of the $(1s^2 2s)^2S^e, M_S = \pm 1/2$ configuration. The most sophisticated final-state wavefunction is a $6C$ wave function, i.e., a product of six two-body Coulomb wave functions, one for each of the six two-body interactions between a nucleus and three free electrons,

$$\Psi_{6C} = \exp(i\vec{k}_1 \cdot \vec{r}_1 + i\vec{k}_2 \cdot \vec{r}_2 + i\vec{k}_3 \cdot \vec{r}_3) \cdot \prod_{i>j} N(\alpha_{ij})$$

$$\times {}_1F_1(i\alpha_{ij}, 1, -i(k_{ij}r_{ij} + \vec{k}_{ij} \cdot \vec{r}_{ij})), \quad (3)$$

where $N(\alpha_{ij})$ is a two-body Coulomb normalization factor and $\alpha_{ij} = Z_i Z_j \mu_{ij}/k_{ij}$ is the Sommerfeld parameter for pair ij with reduced mass μ_{ij} and relative momentum k_{ij}. This is a fully correlated continuum wave function involving all interelectronic coordinates and is a direct generalization of the $3C$ wave function used successfully for photo-double-ionization [12]. A simpler approximation is to use an uncorrelated wave function obtained by omitting the three normalized ${}_1F_1$ functions in Eq. 3 involving the interelectronic distances. The wave function is then simply a product of three electron-nucleus Coulomb wave functions. The direct comparison of photo-triple-ionization cross sections obtained
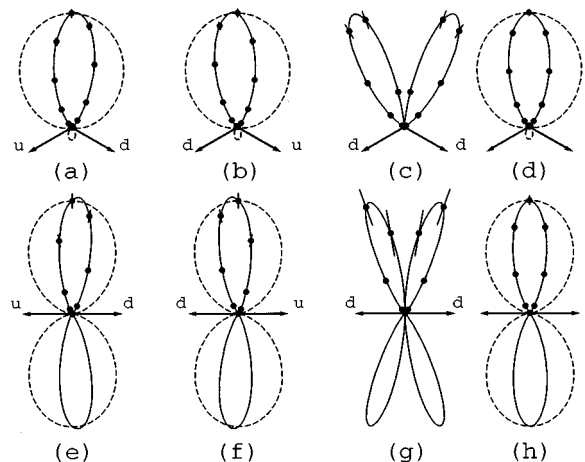

FIG. 1. Angular distribution of electron 3 (with spin up) when electrons 1 and 2 are fixed at relative angles 120° (a)–(d) and 180° (e)–(h). The polarization vector is the vertical axis and the spins are denoted by u (up) and d (down). Dashed curves are for an uncorrelated $3C$ and continuous curves for a correlated $6C$ final state, respectively.

with uncorrelated four-body $3C$ and correlated four-body $6C$ wave functions is made below.

The comparison of cross sections with correlated or uncorrelated wave functions has, however, a deeper significance. It can be shown that in the uncorrelated case additional selection rules hold such that certain measured contributions arise solely from the effect of continuum correlation. The additional selection rules arise essentially from the fact that for a product of single-electron wave functions the cross section vanishes for certain *two-electron* $(\vec{k}_1 s_1, \vec{k}_2 s_2)$ configurations, irrespective of the state of the third electron (i.e., a two-electron selection rule leads to a zero in the three-electron photoionization cross section).

The two main points of this paper, viz., the operation of selection rules and the cross section in the Wannier configuration will be illustrated by sample calculations. The total fragmentation threshold of lithium is at 203.48 eV. In Fig. 1 the cross section is shown for three equal-energy 2-eV electrons and linear photon polarization in the $\hat{z}$ direction. In Figs. 1(e) and 1(f), two electrons are held fixed with equal energies at 180° to each other and with opposite spin. The angular distribution of the third electron is plotted. In accordance with selection rule J the cross section is zero when all three electrons lie in a plane perpendicular to $\hat{\epsilon}$. For the uncorrelated $3C$ wave function, the cross section exhibits a symmetric two-lobe pattern. This $\cos^2(\Theta_3)$ angular pattern is easily understood, since for uncorrelated electrons the initial $(1s^2 2s\uparrow)$ configuration can only result in $(s\uparrow s\downarrow p\uparrow)$, $(s\uparrow p\downarrow s\uparrow)$, or $(p\uparrow s\downarrow s\uparrow)$ configurations. The two latter configurations would give the first two electrons in a $^1P^o$ continuum state, but this probability is zero for $\vec{k}_1 = -\vec{k}_2$ according to the two-electron selection rule C of [5]. Hence only the $(s^2\ ^1S^e, p\ ^2P^o)$ configuration is allowed, giving a $\cos^2(\Theta_3)$ pattern for the third electron. Again, according to the same selection rule, it is clear that the $(s^2\ ^3S^e, p^2 P^o)$ configuration is zero; i.e., when the fixed electrons 1 and 2 have the same spin, the cross section is zero. Already we see that such considerations give an idea of the configurations in which three-electron emission is expected to be favorable.

The most interesting configuration in the threshold region is obtained when the two fixed electrons are measured at a relative angle of 120°. As the third electron, with equal energy, is scanned through the plane containing the other two, the three-electron Wannier configuration is attained when all relative angles are 120°. The observed pattern depends crucially on the orientation of the plane with respect to the linear polarization vector. For example, if $\hat{\epsilon}$ is perpendicular to the plane, then by selection rule A the cross section is identically zero since the parity is odd. By contrast, if $\hat{\epsilon}$ lies in the plane, selection rule J does not operate for the $^2P^o$ state $(\pi + L$ even) considered here and the cross section is finite. In particular, it is finite for the Wannier configuration, in contrast to helium.

The angular distribution of the third electron, when two are held fixed at 120° to the $\hat{\epsilon}$ direction is shown in Figs. 1(a)–1(d), for the uncorrelated $3C$ and fully correlated $6C$ wave functions. For the uncorrelated wave function [dashed line in Figs. 1(a), (b), (e) and (f)] it is readily derived that the cross section is of the form $|(a+b\cos\Theta)|^2$, giving in general a two-lobe structure. The cross sections 1(a) and 1(b) are for the two fixed electrons in a singlet state, with electron 3 having spin up or down, respectively. The results of the Monte Carlo calculation using the $6C$ wave function are also shown, the continuous curve being a smooth fit to the numerical ''data.'' The error bars indicate the true error in convergence with our numerical method. When correlation is switched on, one notes that the strong repulsion due to the other two electrons suppresses the lobe in the lower half-plane in Figs. 1(a) and 1(b) and flattens the lobe in the upper half-plane significantly. The explicit inclusion of electron correlation via terms depending upon the interelectronic distances leads also to a different feature, in that the exchange interaction gives a slightly smaller cross section on the side of the direction $\hat{\epsilon}$ containing the electron with the same spin orientation as electron 3; that is, there is asymmetry with respect to mirror reflection about the direction $\hat{\epsilon}$.

The dependence on electron correlation is even more dramatic when the two fixed electrons are in a triplet state, as in Fig. 1(c). In this case the cross section is identically zero for the uncorrelated wave function, since the independent-electron picture implies applicability of a two-electron selection rule for the two fixed electrons separately. This forbids the triplet state when two electrons are symmetrically disposed to the $\hat{\epsilon}$ direction. By contrast the correlated $6C$ wave function leads to a finite cross section, although in this case the exchange symmetry forces a node precisely at the Wannier configuration.

Since we are interested here in angular distributions, the $3C$ and $6C$ results in Fig. 1 have been normalized to each other. In particular, Figs. 1(a)–1(c) are not drawn to scale, in fact the contribution (c) is roughly two orders of magnitude lower than (a) and (b), reflecting its origin solely due to correlation. Hence the spin-averaged cross section shown in Fig. 1(d) resembles (a) and (b), except of course that the averaging gives a cross section that is symmetric about $\hat{\epsilon}$.

These major features of the spin dependence of crosss sections calculated with correlated wave functions are also to be seen when two electrons are fixed at 180° to each other, as in Figs. 1(e)–1(h). However, here the electron repulsion is equally strong in the upper and lower half-plane, so that the cross section is symmetric with respect to the direction of the two fixed electrons. The left-right asymmetry with respect to $\hat{\epsilon}$ is again evident in Figs. 1(e) and 1(f). The contribution of correlation when the two fixed electrons are in a triplet state (uncorrelated cross section zero) is now a four-lobe structure as shown in Fig. 1(g). The symmetric two-lobe structure of the spin-averaged cross section [Fig. 1(h)] again reflects the dominance of contribution [Figs. 1(e) and 1(f) in which the fixed electrons are in a singlet state.

As with the $3C$ wave function for two electrons, the $6C$ wave function will have erroneous normalization near threshold [13]. However, in the $3C$ case, direct comparison with experimental data [14] has shown that the momentum distributions calculated are completely reliable. Since *absolute* multiply differential cross sections are very difficult to obtain even for two electrons, it is hardly likely that they will be available for three-electron continua in the near future. Experiments to compare with the momentum-distribution cross sections presented here do seem feasible, however.

To summarize, we have presented an analysis of multiply differential cross sections for the $(\gamma, 3e)$ process. We have

established two selection rules (there will probably be more) and have shown that the cross section is finite for the Wannier configuration. We have also shown that final-state correlation leads to two different effects: (a) the population of spin-momentum configurations forbidden in a single-particle picture and (b) a dependence of the symmetry and shape of the cross section on the spin state of the three electrons. Although such spin-resolved measurements probably lie in the distant future, spin-averaged three-electron coincidence measurements to compare with the calculations presented here should soon be available.

[1] G. H. Wannier, Phys. Rev. **90**, 817 (1953); J. W. McGowan and E. M. Clarke, *ibid.* **167**, 43 (1968); H. Kossmann, V. Schmidt, and T. Andersen, Phys. Rev. Lett. **60**, 1266 (1988); J. M. Rost, *ibid.* **72**, 1998 (1994).

[2] S. J. Schaphorst, B. Krässig, O. Schwarzkopf, N. Scherer, and V. Schmidt, J. Phys. B **28**, L233 (1995); P. Lablanquie, J. Mazeau, L. Andric, P. Selles, and A. Huetz, Phys. Rev. Lett. **74**, 2192 (1995); G. Dawber, L. Avaldi, A. G. McConkey, H. Rojas, M. A. MacDonald, and G. C. King, J. Phys. B **28**, L271 (1996).

[3] J. Berakdar, Phys. Rev. A **53**, 2281 (1996).

[4] J. A. R. Samson and G. C. Angel, Phys. Rev. Lett. **61**, 1584 (1988); J. M. Feagin and R. D. Filipczyk, *ibid.* **64**, 384 (1990).

[5] F. Maulbetsch and J. S. Briggs, J. Phys. B **28**, 551 (1995).

[6] S. Diehl *et al.*, Phys. Rev. Lett. **76**, 3915 (1996).

[7] G. C. King and G. Dawber (private communication).

[8] R. Dörner *et al.*, Phys. Rev. Lett. **77**, 1024 (1996).

[9] C. H. Greene and A. R. P. Rau, Phys. Rev. Lett. **48**, 533 (1982); A. D. Stauffer, Phys. Lett. A **91**, 114 (1982).

[10] A. W. Malcherek, F. Maulbetsch, and J. S. Briggs, J. Phys. B **29**, 4127 (1996).

[11] G. P. Lepage, J. Comput. Phys. **27**, 192 (1978).

[12] F. Maulbetsch and J. S. Briggs, J. Phys. B **26**, 1679 (1993).

[13] J. Berakdar and J. S. Briggs, Phys. Rev. Lett. **72**, 3799 (1994).

[14] F. Maulbetsch, M. Pont, J. S. Briggs, and R. Shakeshaft, J. Phys. B **28**, L341 (1995).